The effect of a periodic absorptive strip arrangement on an interior sound field in a room

Joo-Bae Park
Center for Noise and Vibration Control (NOVIC), Department of Mechanical Engineering, Korea Advanced Institute of Science and Technology (KAIST), Science Town, Daejon-shi, 305-701, South Korea

Karl Grosh
Mechanical Engineering and Applied Mechanics, University of Michigan, 2250 G. G. Brown Building, 2350 Hayward Street, Ann Arbor, Michigan 48109-2125

Yang-Hann Kim[a)]
Center for Noise and Vibration Control (NOVIC), Department of Mechanical Vibration, Korea Advanced Institute of Science and Technology (KAIST), Science Town, Daejon-shi, 305-701, South Korea

(Received 10 December 2002; accepted 26 October 2004)

In this paper we study the effect of periodically arranged sound absorptive strips on the mean acoustic potential energy density distribution of a room. The strips are assumed to be attached on the room's surface of interest. In order to determine their effect, the mean acoustic potential energy density variation is evaluated as the function of a ratio of the strip's arrangement period to wavelength. The evaluation demonstrates that the mean acoustic potential energy density tends to converge. In addition, a comparison with a case in which absorptive materials completely cover the selected absorptive plane shows that a periodic arrangement that uses only half of the absorptive material can be more efficient than a total covering, unless the frequency of interest does not coincide with the room's resonant frequencies. Consequently, the results prove that the ratio of the arrangement period to the wavelength plays an important role in the effectiveness of a periodic absorptive strip arrangement to minimize a room's mean acoustic potential energy density. © *2005 Acoustical Society of America.* [DOI: 10.1121/1.1852547]

PACS numbers: 43.55.Dt, 43.55.Ka [MK] Pages: 763–770

I. INTRODUCTION

Much research has been performed regarding how the size and arrangement of absorptive materials affect sound absorption. Parkinson[1] measured the absorption coefficients of absorptive materials in different patterns and different arrangements. His experiments showed that there is a maximum effective spacing that depends on a wavelength; longer waves appear to have a wider spatial influence. He explained that this is mainly because of diffraction. Sabine[2] also noticed this diffraction effect. He noted that there is some discrepancy between what is predicted based on reverberation assumptions and what is actually measured, and showed that a localized absorption often produces this discrepancy due to diffraction. Chrisler[3] experimentally studied the effect of the size of the sample on the absorption coefficient measurement. His experiments show that the measured absorption coefficient of a small sample is greater than the coefficient of a large sample, and the measured absorption coefficient converges as the sample size increases. Ramer[4] experimentally studied the effect of varying the width of an absorbing strip and the effect of its location in a reverberation chamber. He concluded that the narrower the strip, the greater the absorption coefficient. Harris[5] reported that absorption characteristics vary, depending on where absorptive patches are placed. He experimentally showed that absorption is greatest if the patches are placed where the pressure is greatest. Investigations on sound absorption by patches (or strips) conducted by Pellam,[6] Levitas and Lax,[7] Cook,[8] and Northwood, Geisaru, and Medcof[9] had similar conclusions. These studies showed analytically that as the absorption coefficient increases, the absorptive patch (or strip) is made smaller. Daniel[10] experimentally showed that not only does absorption increase proportional to the size of the absorptive material, but also that its edges tend to be longer. Mechel[11,12] used an iterative method and variational formulation[7,13] to construct two approximate solutions to evaluate absorption for finite-sized absorbers. With the approximate solutions, he built expressions for the radiation impedance of the absorbing strip and rectangles. Thomasson[14] derived a general statement about the absorption of a locally reacting patch with an arbitrary shape. He evaluated the pressure on the absorber by using the variational principle, and then constructed a new statistical absorption coefficient of which the magnitude is always less than 1. The absorption coefficient, instead of using incident power related to the infinite absorber, is defined as the ratio between absorbed and available power.

Especially important to this research are the studies by Bruijn,[15,16] Takahashi,[17] and Mechel[18] that investigated the effect of periodically arranged absorptive materials on sound reduction and analytically evaluated excess absorption properties by considering both a periodically absorbing uneven surface and a flat surface. Takahashi's experimental result

[a)]All correspondences must be sent to Yang-Hann Kim (yanghannkim@kaist.ac.kr)

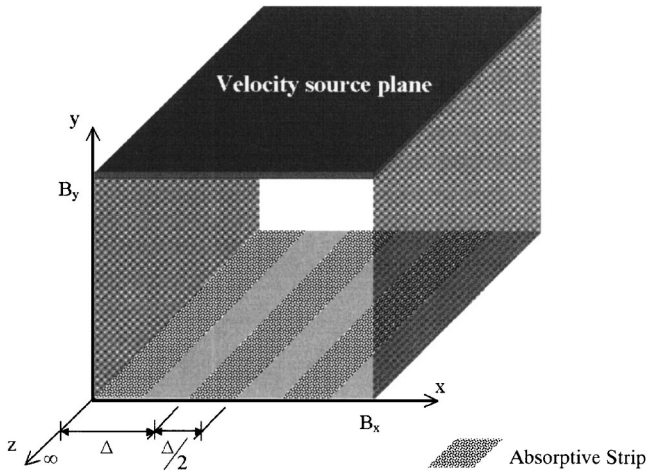

FIG. 1. A parallelepiped enclosure of an infinite length in the z direction. On the plane at $y=0$, absorptive strips of infinite length and width $\Delta/2$ are arranged periodically. The arrangement period is defined as Δ.

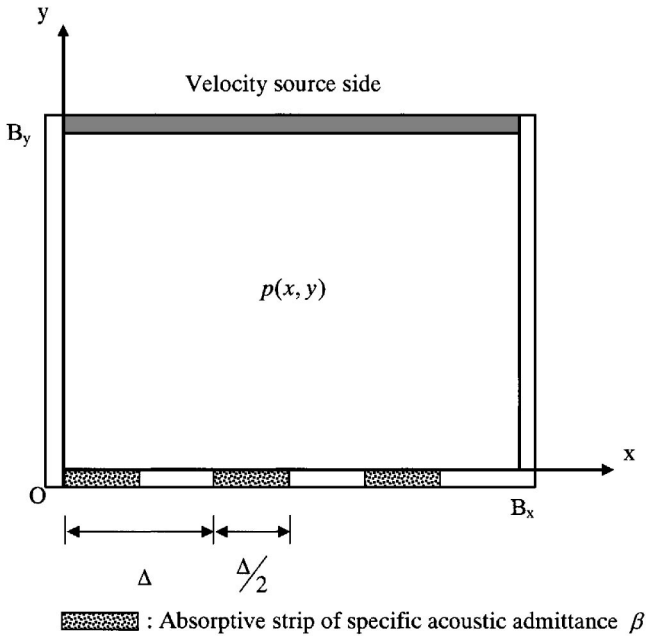

FIG. 2. Cross sectional view of Fig. 1. The source side at $y=B_y$ vibrates in the velocity of $u_y=f(x)e^{j\omega t}$. In this case, there are three absorptive strips on the absorptive plane at $y=0$.

complemented analytical evaluations for the periodic absorber on the flat surface. Mechel,[18] by introducing Hartree harmonics to distinguish the scattered field from the periodic absorbers, evaluated the absorption, the reflection coefficient, the directivity and field pressure patterns of various surfaces, such as plates with periodic grooves filled with absorber material, empty grooves with an absorbing ground, and perforated covers on porous absorbers. In these studies, Bruijn, Takahashi, and Mechel[18] assume that the extensions of the absorbers are infinite. Holmberg, Hammer, and Nilsson[19] used a variational formulation to evaluate the combined absorption characteristics of a finite-size absorber of arbitrary shape with subareas that are arranged in a specific pattern. As a result, in their study, separating the subareas increases the statistical absorption coefficient, which is a function of both the surface impedance of the absorbers and the radiation impedance. They verified their evaluation by a comparison with the measurement result.

These previous researches mainly studied how the absorption of a surface varies due to the shape and arrangement of the absorptive material. However, they did yet explore to understand how the arrangement affects the acoustic potential energy density of an enclosure. In this paper we seek to address this important practical consideration. This study's theoretical result indicates how the sound absorptive material can best be arranged to obtain the desired acoustic potential energy reduction.

II. PROBLEM STATEMENT

The objective of this study is to investigate the effect of periodic absorptive strip arrangement on an interior sound field. Periodic absorptive strip arrangement on a wall is depicted in Fig. 1. Mathematically, this means that we have to solve a mixed boundary value problem.[20] The analytic solution for a general sound field, which has a mixed boundary condition, cannot be obtained easily. It is significant that our aim is to see the effect of the absorptive strip arrangement on an acoustic potential energy density, not to find a general three-dimensional solution that describes details of the interior sound field. So, we attempt to use a two-dimensional analytic solution for studying the relation. Figure 1 shows a parallelepiped enclosure where absorptive strips, with a specific acoustic admittance β of 1, are arranged periodically on the rigid plane at $y=0$. This specific acoustic admittance β is defined as the ratio of the normal particle velocity to the sound pressure on the absorptive material, times ρc, where ρ is the density and c is the speed of sound. The plane at $y=B_y$ vibrates harmonically in a prescribed manner. The other two vertical planes at $x=0$, B_x are assumed to be rigid. The parallelepiped enclosure's z-directional length is assumed to be infinite so that the interior sound field does not vary in the z direction. Accordingly, the interior sound field can be considered to be two-dimensional, as depicted in Fig. 2.

Figure 2 shows a two-dimensional rectangular enclosure; there are two rigid sides at $x=0$, B_x: a source side at $y=B_y$, and an absorptive side at $y=0$. The arrangement period Δ can be written as

$$\Delta=\frac{B_x}{L}, \tag{1}$$

where L is the total number of absorptive material strips. Consequently, L is always an integer variable. The width of the absorptive strip is assumed to be $\Delta/2$. Therefore, regardless of L, the following relation always holds:

$$\frac{total\ \ width\ \ of\ \ absorptive\ \ strip}{B_x}=\frac{1}{2}. \tag{2}$$

It is noteworthy that the constraint of Eq. (2) essentially preserves the total absorptive material usage, regardless of period changes in the absorptive strip's arrangement. This enables us to observe the acoustic potential energy density variation due to the Δ change.

Then let us define dimensionless variables as $\tilde{\rho}=\rho/\rho_0$, $\tilde{c}=c/c_0$, $\tilde{p}=p/\rho_0 c_0^2$, $\tilde{x}=x/\lambda$, $\tilde{y}=y/\lambda$, $\tilde{B}_x=B_x/\lambda$, $\tilde{B}_y=B_y/\lambda$, $\tilde{k}=k\cdot\lambda$ (i.e., $\tilde{k}=2\pi$), and $\tilde{\Delta}=\Delta/\lambda$, where c_0 and ρ_0 are phase speed and density of air, respectively. Here, c and ρ are phase speed and density of air so that $\tilde{\rho}=1$ and $\tilde{c}=1$. In order to verify the effect of the wavelength on a sound field with a periodic absorptive strip arrangement, the wavelength λ scales every length variable, such as coordinates and wave number.

Substituting these dimensionless variables into the Helmholtz equation and boundary conditions yield

$$\left(\frac{\partial^2}{\partial\tilde{x}^2}+\frac{\partial^2}{\partial\tilde{y}^2}+\tilde{k}^2\right)\tilde{p}(\tilde{x},\tilde{y})=0, \tag{3}$$

$$\frac{\partial\tilde{p}}{\partial\tilde{x}}=0, \quad \text{at } \tilde{x}=0, \tag{4}$$

$$\frac{\partial\tilde{p}}{\partial\tilde{x}}=0, \quad \text{at } \tilde{x}=\tilde{B}_x, \tag{5}$$

$$\frac{\partial\tilde{p}}{\partial\tilde{y}}=\tilde{g}(\tilde{x}), \quad \text{at } \tilde{y}=0, \tag{6a}$$

where

$$\tilde{g}(\tilde{x})=\begin{cases} j2\pi\beta\tilde{p}, & l\tilde{\Delta}<\tilde{x}\leqslant(l+0.5)\tilde{\Delta},\ l=0,1,2,...,L, \\ 0, & (l+0.5)\tilde{\Delta}<\tilde{x}\leqslant(l+1)\tilde{\Delta},\ l=0,1,2,...,L, \end{cases} \tag{6b}$$

$$\frac{\partial\tilde{p}}{\partial\tilde{y}}=-j2\pi\tilde{\rho}\tilde{c}\cdot\tilde{f}(\tilde{x}), \quad \text{at } \tilde{y}=\tilde{B}_y, \tag{7}$$

where the function $\tilde{f}(\tilde{x})$ expresses the dimensionless velocity that is defined as $\tilde{f}(\tilde{x})=f(\tilde{x})/c_0$. The function $\tilde{g}(\tilde{x})$ describes the periodic absorptive strip arrangement on the rigid side at $y=0$. These dimensionless forms of the governing equation and boundary conditions completely describe the problem we want to study. The next step is to solve this mathematical problem and obtain useful information that can provide us with guidelines for obtaining the desired acoustic energy reduction by using a periodic sound absorptive strip arrangement.

III. SOLUTION METHOD

A solution that completely describes the enclosure's interior sound field can be obtained by summing the modal functions that satisfy the prescribed boundary conditions. It is, however, essential to first get the modal functions. For example, a mixed boundary condition, which is illustrated in Fig. 1, makes it difficult to find normal modes in the y direction. In the following section we explain how to get an approximate solution that meets our objectives.

A. Truncated approximate solution

First, we apply the method of separation of variable to Eq. (3). This gives the following general solution:

$$\tilde{p}(\tilde{x},\tilde{y})=(Ce^{-j\tilde{k}_x\tilde{x}}+De^{j\tilde{k}_x\tilde{x}})(Ee^{-j\tilde{k}_y\tilde{y}}+Fe^{j\tilde{k}_y\tilde{y}}), \tag{8}$$

where C, D, E, F are arbitrary constants. The propagation constants $\tilde{k}_x$ and $\tilde{k}_y$ satisfy the following relation:

$$\tilde{k}_x^2+\tilde{k}_y^2=\tilde{k}^2, \tag{9}$$

where the dimensionless wave number is $\tilde{k}=2\pi$.

The homogeneous Neumann boundary condition, on the sides of $x=0$ and $x=B_x$, determines the eigenvalue and eigenfunctions in the x direction; substituting Eq. (8) for $\tilde{p}$ in Eqs. (4) and (5) gives the following eigenvalues:

$$\tilde{k}_{xn}=\frac{n\pi}{\tilde{B}_x}, \quad n=0,1,2,.... \tag{10}$$

The corresponding eigenfunctions are

$$\phi_n(\tilde{x})=\epsilon_n\cos(\tilde{k}_{xn}\tilde{x}), \quad n=0,1,2,..., \tag{11a}$$

where

$$\epsilon_n=\begin{cases} 1, & n=0, \\ \sqrt{2}, & n=1,2,3,.... \end{cases} \tag{11b}$$

Therefore, the general solution (8) can be rewritten as

$$\tilde{p}(\tilde{x},\tilde{y})=\sum_{n=0}^{\infty}\phi_n(x)(E_ne^{-j\tilde{k}_{yn}\tilde{y}}+F_ne^{j\tilde{k}_{yn}\tilde{y}}), \tag{12a}$$

where

$$\tilde{k}_{xn}^2+\tilde{k}_{yn}^2=(2\pi)^2. \tag{12b}$$

Because $\tilde{p}(\tilde{x},\tilde{y})$, given by Eq. (12), always satisfies the governing equation (3) and the rigid boundary conditions at $\tilde{x}=0$ and $\tilde{x}=\tilde{B}_x$, all that remains is to find the unknown coefficients E_n and F_n that satisfy the boundary conditions $\tilde{y}=0$ and $\tilde{y}=\tilde{B}_y$, respectively. It is noteworthy that we have to somehow limit our summation of Eq. (12) to a finite number N. This can be simply done by limiting the sum until it converges; in other words, when E_n and F_n tend to zero as n goes to $N-1$. Therefore, Eq. (6) can be rewritten as

$$\sum_{n=0}^{N-1}\phi_n(\tilde{x})[j\tilde{k}_{yn}(-E_n+F_n)]=\tilde{g}(\tilde{x}). \tag{13}$$

Here $\tilde{g}(x)$ [Eq. (6b)] has to be rewritten as

$$\tilde{g}(\tilde{x})=\begin{cases} j2\pi\beta\sum_{n=0}^{N-1}\phi_n(\tilde{x})(E_n+F_n), & l\tilde{\Delta}<\tilde{x}\leqslant(l+0.5)\tilde{\Delta},\ l=0,1,2,...,L, \\ 0, & (l+0.5)\tilde{\Delta}<\tilde{x}\leqslant(l+1)\tilde{\Delta},\ l=0,1,2,\ldots,L. \end{cases} \tag{14}$$

Also, substituting the finite form of Eq. (12) to another boundary condition, Eq. (7), yields

$$\sum_{n=0}^{N-1}\phi_n(\tilde{x})[j\tilde{k}_{yn}(-E_n e^{-j\tilde{k}_{yn}\tilde{B}_y}+F_n e^{j\tilde{k}_{yn}\tilde{B}_y})] = -j2\pi\tilde{\rho}\tilde{c}\cdot\tilde{f}(\tilde{x}). \tag{15}$$

It is also noteworthy that the $\phi_n(\tilde{x})$ and $\tilde{f}(\tilde{x})$ in Eqs. (13) and (15) are prescribed; therefore, we have $2N$ number of unknowns E_n and F_n. Henceforth, $2N$ number of linear algebraic equations are required to determine unknown coefficients E_n and F_n. Applying the method of weighted residual[21] to Eqs. (13) and (15) provides the set of $2N$ linear algebraic equations. If the approximate solution (a finite sum instead of an infinite sum) exactly satisfies the boundary condition at $\tilde{y}=0$ and $\tilde{y}=\tilde{B}_y$, then Eqs. (13) and (15) can be rewritten as

$$\int_0^{\tilde{B}_x}\left(\sum_{n=0}^{N-1}\phi_n(\tilde{x})[j\tilde{k}_{yn}(-E_n+F_n)]-\tilde{g}(\tilde{x})\right)w_i(\tilde{x})d\tilde{x}=0, \tag{16}$$

$$\int_0^{\tilde{B}_x}\left(\sum_{n=0}^{N-1}\phi_n(\tilde{x})[j\tilde{k}_{yn}(-E_n e^{-j\tilde{k}_{yn}\tilde{B}_y}+F_n e^{j\tilde{k}_{yn}\tilde{B}_y})] + j2\pi\tilde{\rho}\tilde{c}\cdot\tilde{f}(\tilde{x})\right)h_i(\tilde{x})d\tilde{x}=0, \tag{17}$$

where $w_i(\tilde{x})$ and $h_i(\tilde{x})$ are the weight functions that are defined in the range of $0\leqslant\tilde{x}\leqslant\tilde{B}_x$. It is noteworthy that Eq. (16) essentially has $2L$ different integral intervals due to the periodic absorptive strip arrangement. Therefore, if we apply the weighting function $w_i(\tilde{x})$ into Eq. (16), then we have $2L$ linear algebraic equations. Those weighting functions, which are linearly independent, can be defined as

$$w_i(\tilde{x})=\sin\left(\frac{2(i+1)\pi}{\Delta}\tilde{x}\right),\quad i=0,1,2,\cdots\left(\frac{N}{2L}-1\right), \tag{18}$$

$$h_i(\tilde{x})=\epsilon_i\cos(\tilde{k}_{xi}\tilde{x}),\quad i=0,1,2,...(N-1), \tag{19}$$

where ϵ_i is the same as that used in Eq. (11b). In order to use the orthogonal property of the eigenfunction when we calculate Eq. (17), $h_i(\tilde{x})$ is written in the same form of eigenfunction $\phi_n(\tilde{x})$. Finally, solving the set of $2N$ linear algebraic equations gives E_n and F_n, which make the approximate solution satisfy the boundary conditions at $\tilde{y}=0$ and $\tilde{y}=\tilde{B}_y$.

B. Accuracy of the approximate solution

The approximate solution, which is a truncated form of Eq. (12), has an error because it does not exactly satisfy the boundary conditions [Eqs. (13) and (15)]. Equation (15), which expresses the boundary condition at $\tilde{y}=\tilde{B}_y$, essentially decomposes $\tilde{f}(\tilde{x})$ in terms of eigenfunctions $\{\phi_n(\tilde{x})\}_{n=0}^{N-1}$. Therefore, if we select the function $\tilde{f}(\tilde{x})$ as a combination of eigenfunctions $\{\phi_n(\tilde{x})\}_{n=0}^{N-1}$, then it satisfies the boundary condition at $\tilde{y}=\tilde{B}_y$ and we have an error only on the absorptive side at $\tilde{y}=0$. This error determines the solution's accuracy.

The error is defined in two different ways. One definition evaluates the relative error due to the admittance discrepancy. That is,

$$\bar{\beta}_{\text{error}}=\frac{1}{0.5\tilde{B}_x|\beta_{in}|}\sum_{l=0}^{L-1}\int_{l\tilde{\Delta}}^{(l+0.5)\tilde{\Delta}}|\beta(\tilde{x})-\beta_{in}|d\tilde{x}, \tag{20}$$

where β_{in} is the given constant admittance and $\beta(\tilde{x})$ is the admittance reconstructed based on the approximate solution. Therefore, $\bar{\beta}_{\text{error}}$ refers to how well the approximate solution, compared to β_{in}, satisfies the boundary condition on the absorptive strip. It is important that Eq. (20) is applied only to surfaces where absorptive strips are attached.

The other definition is for the error where no absorptive strips are arranged. That is,

$$\bar{R}_{\text{error}}=\frac{1}{0.5\tilde{B}_x|\tilde{U}_0|}\sum_{l=0}^{L-1}\int_{(l+0.5)\tilde{\Delta}}^{(l+1)\tilde{\Delta}}|\tilde{u}_y(\tilde{x})|d\tilde{x}, \tag{21}$$

where $\tilde{U}_0$ is the given dimensionless source velocity magnitude [i.e. $|\tilde{f}(\tilde{x})|$] and $\tilde{u}_y(\tilde{x})$ is the reconstructed dimensionless y-direction velocity on the rigid wall. Therefore, $\bar{R}_{\text{error}}$ refers to how well the approximate solution, compared to the source velocity magnitude $|\tilde{U}_0|$, satisfies the rigid wall condition between absorptive strips. These two measures of error essentially evaluate the performances of the truncated approximate solutions in two ways: one has to do with admittance and the other is related to the rigid boundary condition.

We now have a solution method and measures that evaluate how well the solution method works for the nondimensional mixed boundary value problem. Therefore, the next step is to find practical guidelines for quieting an enclosure using the periodic absorptive strip arrangement.

IV. DIMENSIONLESS PARAMETER STUDY

In order to determine the effect of a periodic absorptive strip arrangement, the dimensionless mean acoustic potential energy density of the entire cross section, which is illustrated in Fig. 2, is evaluated while changing the absorptive strip's arrangement period but while preserving the constraint of Eq. (2). As explained, the constraint of Eq. (2) means that the total area of the absorptive material is fixed as a constant.

In order to investigate the effect of the cross sectional shape, the side length ratio $\delta(=B_y/B_x)$ is introduced. Then,

for δ=0.01, 0.1, 1, 10, and 100 the effect of the arrangement period change is investigated for each. The area of the cross section, for each δ, is considered to be $1 \leqslant \tilde{A} \leqslant 100$, where $\tilde{A}=\tilde{B}_x\tilde{B}_y$. Consequently, $\tilde{A}$ means the dimensionless area that is normalized by λ^2. It is also noteworthy that the length ratio δ can be any positive value for the same area $\tilde{A}$. The total number of the basis functions of Eq. (12) is selected in such a way as to make the solution sufficiently accurate and considers computational capability, namely, $N=800$. The source side velocity $\tilde{f}(\tilde{x})$, to make a numerical evaluation simple, is defined as a constant (i.e, $\tilde{f}(\tilde{x})=0.001$). There can be many possible choices for selecting the admittance of the absorptive material. However, the specific acoustic admittance of the absorptive strip is defined as β=1 (i.e., as an impedance matching boundary condition). This choice maximizes the absorption difference between the absorptive strip and the rigid wall so that we can clearly observe the effect of the periodic arrangement.

A. Cost function and parameters

The cost function, which depends on the absorptive material arrangement change, is defined as the dimensionless mean acoustic potential energy density $\tilde{e}_p$. Specifically, the cost function $\tilde{e}_p$ of an entire rectangular cross section with a normalized area of $\tilde{A}$, using the truncated approximate solution of Eq. (12), can be defined as

$$\begin{aligned}\tilde{e}_p &= \frac{1}{4\tilde{A}\tilde{\rho}\tilde{c}^2}\int_0^{\tilde{B}_y}\int_0^{\tilde{B}_x}|\tilde{p}(\tilde{x},\tilde{y})|^2 d\tilde{x}\,d\tilde{y} \\ &= \frac{1}{4\tilde{A}\tilde{\rho}\tilde{c}^2}\sum_{n=0}^{N-1}\left[\tilde{B}_y(|E_n|^2+|F_n|^2)\right. \\ &\quad \left. +2\int_0^{\tilde{B}_y}\mathrm{Re}(E_n^* F_n e^{j2\tilde{k}_{yn}\tilde{y}})d\tilde{y}\right], \end{aligned} \tag{22}$$

where* is the complex conjugate. This means that the total dimensionless acoustic potential energy is divided by the dimensionless area: an average acoustic potential density in the rectangular cross section.

The parameters are a dimensionless variable $\tilde{A}$ that refers to a normalized room volume of a unit length in the z direction, and a dimensionless integer variable $L(=B_x/\Delta)$ that refers to the number of absorptive strips on the absorptive side at $\tilde{y}=0$. The larger L is, for a constant B_x, the smaller is the absorptive strip's arrangement period Δ. It is significant that a noninteger L violates the constraint of Eq. (2). On the contrary, integer values of L mean that the total usage of absorptive materials is always half of an absorptive area defined at $y=0$, independent of the arrangement period Δ change.

B. Results and discussion

Figures 3, 4, 5, 6, and 7 show the cost function $\tilde{e}_p$ variation for δ=0.01, 0.1, 1, 10, and 100, respectively. Here, the periodic arrangement change is represented by L, i.e., by the number of absorptive strips on $y=0$. In Figs. 3–7, the normalized acoustic potential energy density level E_L is defined as

$$E_L = 10\log_{10}\left(\frac{\tilde{e}_p}{\tilde{e}_{po}}\right), \tag{23}$$

where $\tilde{e}_{po}$ means $\tilde{e}_p$ when the absorptive material totally covers the plane at $y=0$. Therefore, in the case of $\tilde{e}_{po}$, the total absorptive material usage is double that of the periodic arrangement. Due to the constraint of Eq. (2), regardless of the period change, the periodic arrangement covers only half of the plane at $y=0$. In order to determine the efficiency of the periodic arrangement with respect to an extreme case, the acoustic potential energy density is normalized by $\tilde{e}_{po}$. Also, there are additional contour lines of $E_L=0$ in Figs. 3–7, which make it easy to find where the region has $\tilde{e}_p$ that is smaller than $\tilde{e}_{po}$.

Figure 3 shows the case of δ=0.01, in which E_L variation is a function of $\tilde{A}$ and L ($1 \leqslant \tilde{A} \leqslant 100$ and $1 \leqslant L \leqslant 20$). In Fig. 3(b), zero level contour lines divide the result into two regions: the darker region of $E_L>0$ and the brighter region

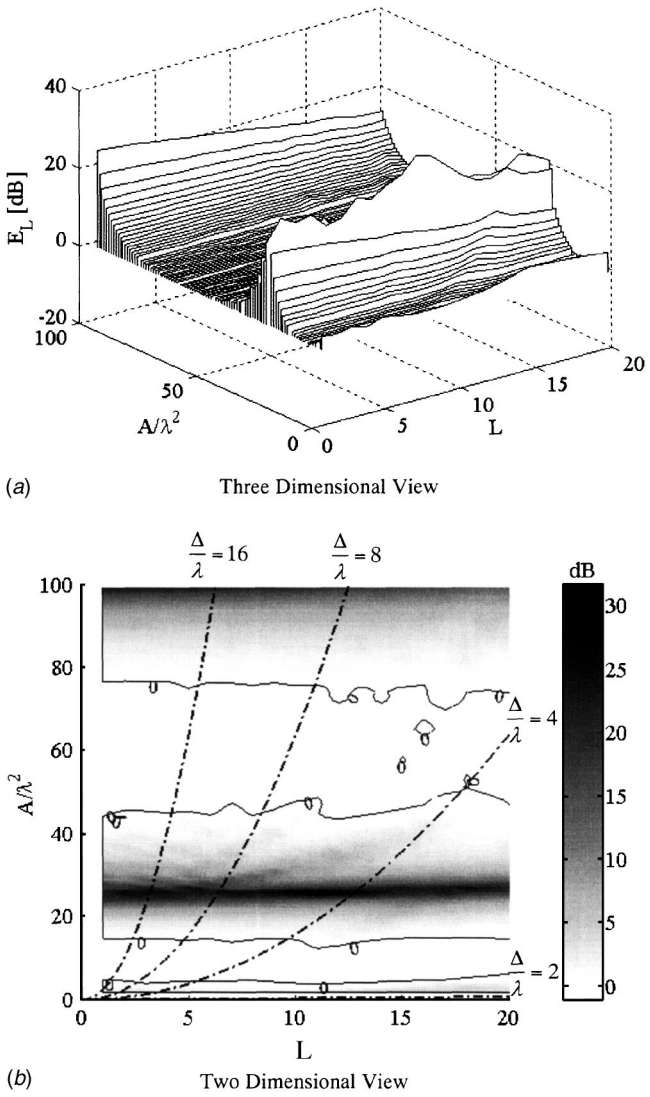

FIG. 3. Normalized acoustic potential energy density level E_L variation as the function of both $\tilde{A}$ and L when δ=0.01.

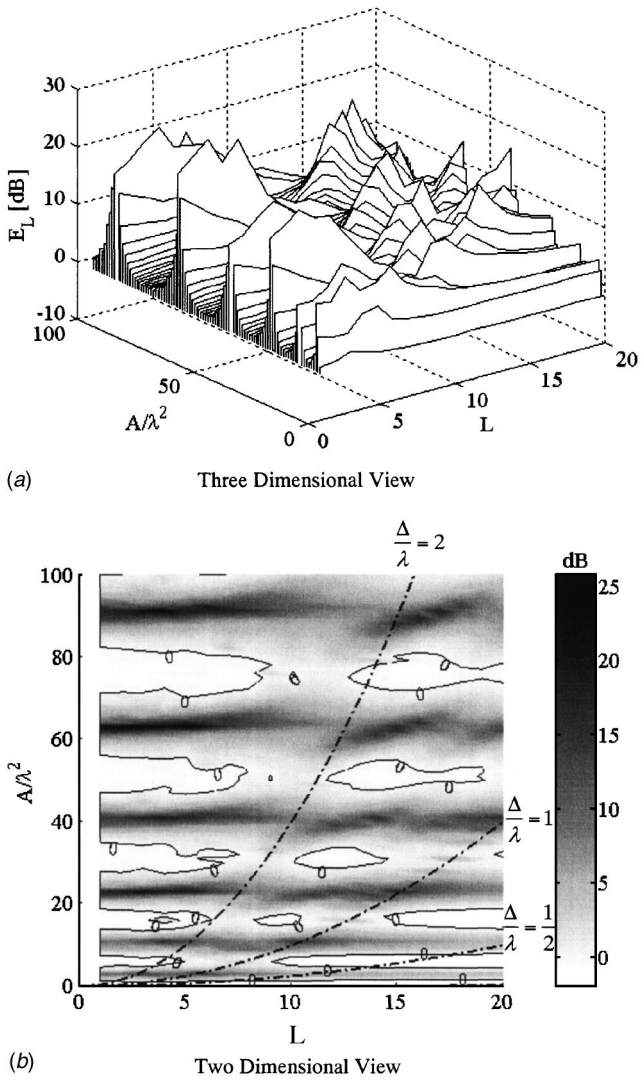

FIG. 4. Normalized acoustic potential energy density level E_L variation as the function of both $\tilde{A}$ and L when $\delta=0.1$.

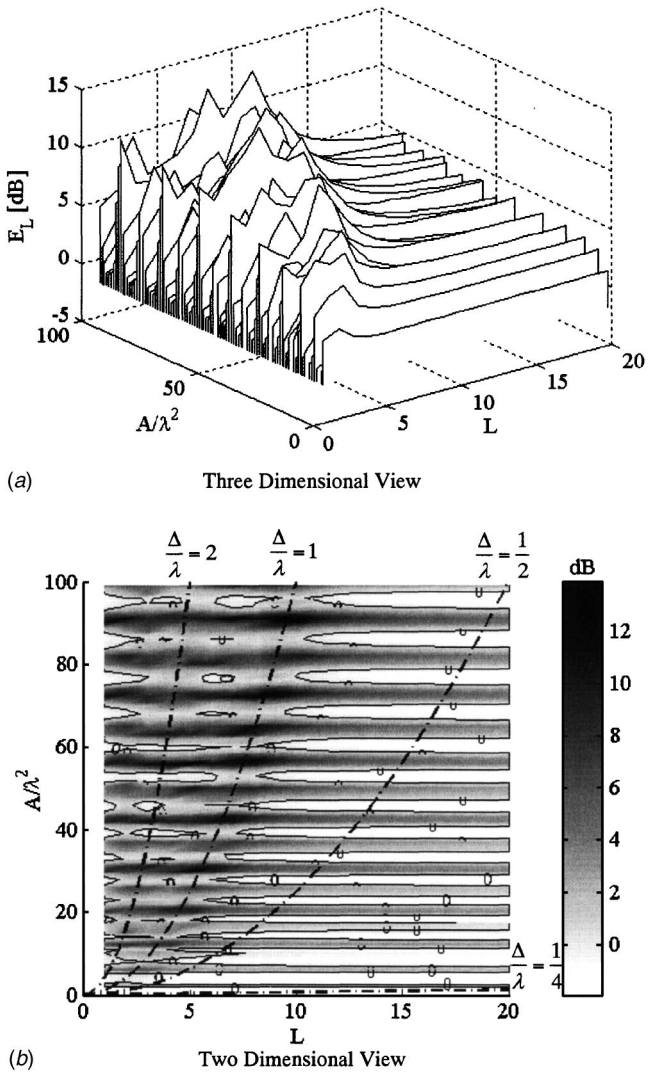

FIG. 5. Normalized acoustic potential energy density level E_L variation as the function of both $\tilde{A}$ and L when $\delta=1$.

of $E_L<0$. The region of $E_L<0$ proves that as long as the sound field is not a case of resonance, a periodic arrangement can be more efficient than a fully covered case. Even though the difference from $\tilde{e}_{po}$ is not large, the regions of $E_L<0$ are distinctly observed. Dark bands in Fig. 3, which mean higher E_L, are shown near the case of $B_y/\lambda=n/2$, where n is a nonzero integer. This corresponds to the case in which the side length B_y of the enclosure is in integer multiples of half wavelengths, i.e., resonances. In order to observe the effect of a Δ/λ change in the periodic absorptive material arrangement, three dash–dotted lines of constant Δ/λ are added to Fig. 3. Here, Δ/λ means the ratio between the absorptive strip arrangement period and the wavelength. It is also noteworthy that L and $\tilde{A}$ have a quadratic relation of $\tilde{A}=\delta\cdot(\Delta/\lambda)^2\cdot L^2$. Therefore, the relations of constant $\Delta/\lambda=16$, 8, 4, and 2 are expressed as individual quadratic curves in Fig. 3. Here, Fig. 3 does not show explicitly any dependency of E_L on the Δ/λ change. However, in the consecutive evaluations of $\delta=0.1$, 1, 10, and 100, we can observe that Δ/λ is a major parameter on the E_L variation.

Figure 4 depicts the case of $\delta=0.1$. This case is similar to that in Fig. 3 as the region of $E_L<0$ and the darker bands of the resonance region are again observed. Unlike Fig. 3, however, due to the change of δ, there are a greater number darker bands and a region of $E_L<0$ appears between them. Specifically, due to the enlarged δ, for the same range of $\tilde{A}$, the domain of B_y is increased but the domain of B_x is decreased. In addition, Fig. 4 clearly shows the dependency on the Δ/λ change. The dash-dotted lines of $\Delta/\lambda=2$ and $\Delta/\lambda=1$, which are different from Fig. 3, break the regions of $E_L<0$. This result assures that the ratio of the arrangement period to the wavelength, i.e. Δ/λ, affects the variation of the acoustical potential energy density.

Next, in Fig. 5, which shows $\delta=1$ (i.e, a square cross section), the number of darker bands is greater and the region of $E_L<0$ is denser than in Figs. 3 and 4, but the overall trend is similar to that in Fig. 4. The lines of $\Delta/\lambda=2$ and $\Delta/\lambda=1$ break the region of $E_L<0$, and the region between $\Delta/\lambda=2$ and $\Delta/\lambda=1$ seems to be a transition region. In addition, compared to Figs. 3 and 4, Fig. 5 shows more distinctly the E_L dependency on Δ/λ. The line of $\Delta/\lambda=1$ acts as a borderline that divides the variation trend of E_L. The region where $\Delta/\lambda<1$, the overall E_L variation due to L change regardless

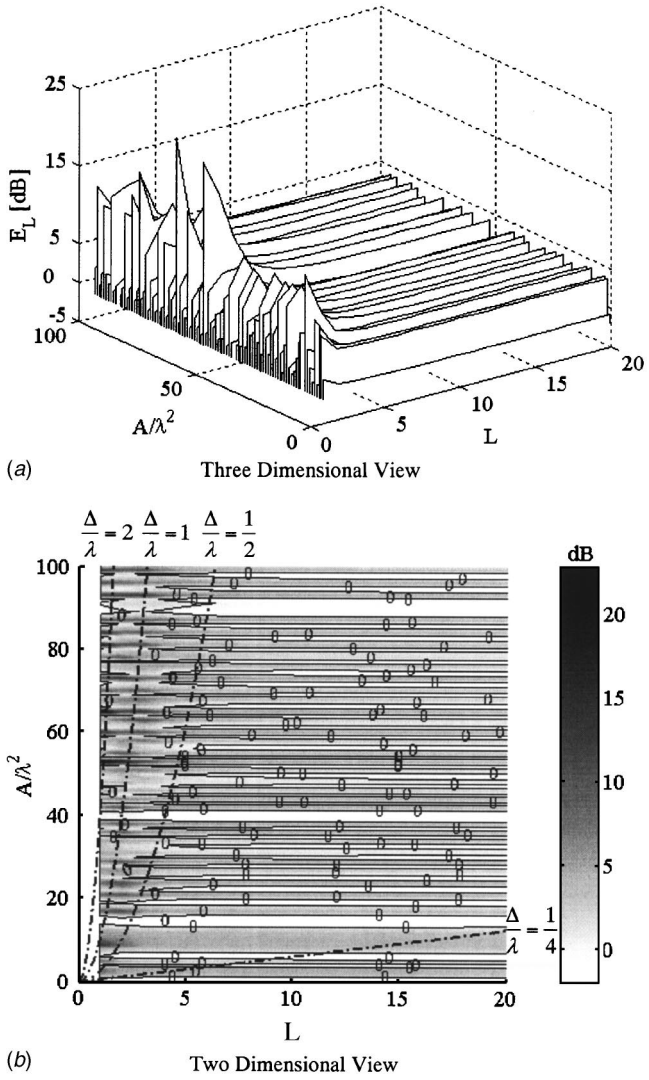

FIG. 6. Normalized acoustic potential energy density level E_L variation as the function of both $\tilde{A}$ and L when $\delta=10$.

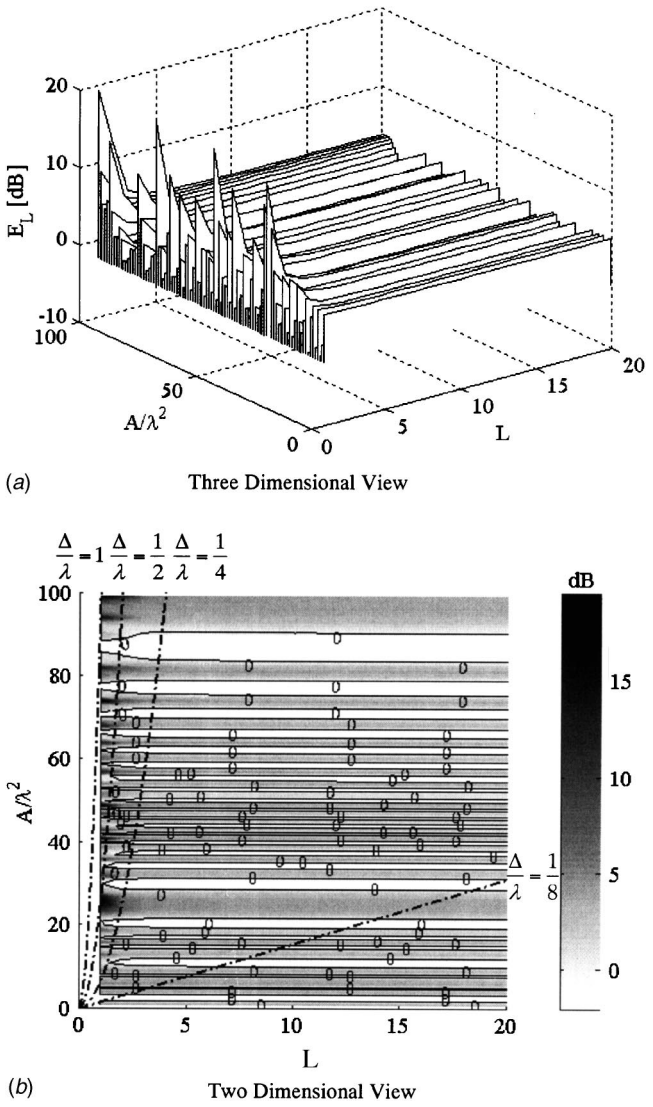

FIG. 7. Normalized acoustic potential energy density level E_L variation as the function of both $\tilde{A}$ and L when $\delta=100$.

of $\tilde{A}$ converges to some constant value. Whether $\tilde{A}$ is resonance or not, this stable condition is applied in the same way.

Figure 6 shows the case of $\delta=10$ and has a similar result. Even though the region of $E_L<0$ is denser than the case of $\delta=1$, the line of $\Delta/\lambda=1$ divides the E_L variation as in Fig. 5. As explained in Fig. 4, the larger is δ, the longer is B_y. Therefore, compared to the case of the smaller δ, more resonance lines are observed in the same range of $1\leqslant\tilde{A}\leqslant100$.

Finally, Fig. 7 shows the case where $\delta=100$. In this case, as depicted in Fig. 7(b), all the evaluation cases correspond where $\Delta/\lambda<1$. As a result, except for the region near $L=1$, the variation of E_L converges rapidly. The consecutive results of Figs. 5–7 stress that two conditions should be satisfied to make $\tilde{e}_p$ less than $\tilde{e}_{po}$ through the periodic absorptive material arrangement: the sound field should not be resonance, and the ratio should be $\Delta/\lambda<1/2$.

The accuracy of Figs. 3–7 is evaluated by Eqs. (20) and (21). Table I shows mean errors for the five different cases of $\delta=0.01$, 0.1, 1, 10, and 100. The range of the admittance boundary condition reconstruction error is $1.4\times10^{-02}\leqslant\overline{\beta}_{\text{error\_mean}}\leqslant2.3\times10^{-02}$, and the range of the rigid wall boundary condition reconstruction error is $2.1\times10^{-02}\leqslant\overline{R}_{\text{error\_mean}}\leqslant2.9\times10^{-02}$. Therefore, $\max(\beta_{\text{error\_mean}})$ is 2.3% and $\max(R_{\text{error\_mean}})$ is 2.9%. These errors are assumed to be acceptable.

V. CONCLUSION

In this study we focus on how the periodic absorptive strip arrangement affects an interior sound field's mean acoustic potential energy density. Specifically, throughout a

TABLE I. Mean admittance and rigid wall bondary condition reconstruction error for five different cross sectional shapes with side ratio $\delta=0.01$, 0.1, 1, 10, and 100, respectively.

δ	$\overline{\beta}_{\text{error\_mean}}$	$\overline{R}_{\text{error\_mean}}$
0.01	2.3×10^{-02}	2.9×10^{-02}
0.1	2.2×10^{-02}	2.9×10^{-02}
1	1.5×10^{-02}	2.0×10^{-02}
10	1.5×10^{-02}	2.1×10^{-02}
100	1.4×10^{-02}	2.1×10^{-02}

parameter study for five different cross sectional shapes with side ratios of δ=0.01, 0.1, 1, 10, and 100, the relation between the ratio Δ/λ of the arrangement period to the wavelength and the enclosure's mean acoustic potential energy density $\tilde{e}_p$ is investigated. Also, in order to determine the efficiency of the periodic absorptive strip arrangement, every $\tilde{e}_p$ of the periodic arrangement is compared to a case in which the surface was fully covered by strips. As a result, the parameter study shows that the sound absorption performance is not simply a function of how much absorptive material is used. It demonstrates that the periodic absorptive strip arrangement is more efficient, if the frequency of interest is not one of the room's resonance frequencies and if the ratio of the arrangement period Δ to wavelength λ is less than 0.5, i.e. $\Delta/\lambda<1/2$. On the contrary, at resonance, $\tilde{e}_p$ of the periodic arrangement is always larger than in the totally covered case.

ACKNOWLEDGMENTS

This study was partially supported by the NRL (National Research Laboratory) of KISTEP (Korea Institute of Science & Technology Evaluation and Planning) and by BK21 (Brain Korea 21), the Ministry of Education & Human Resources Development of Korea.

[1] J. S. Parkinson, ''Area and pattern effects in the measurements of sound absorption,'' J. Acoust. Soc. Am. **2**, 112–122 (1930).
[2] P. E. Sabine, ''What is measured in sound absorption measurement,'' J. Acoust. Soc. Am. **6**, 239–245 (1935).
[3] V. L. Chrisler, ''Dependence of sound absorption upon the area and distribution of the absorbent material,'' J. Res. Natl. Bur. Stand. **13**, 169–187 (1934).
[4] L. G. Ramer, ''The absorption of strips, effects of width and location,'' J. Acoust. Soc. Am. **12**, 323–326 (1941).
[5] C. M. Harris, ''The effect of position on the acoustical absorption by a patch of material in a room,'' J. Acoust. Soc. Am. **17**, 242–244 (1946).
[6] J. R. Pellam, ''Sound diffraction and absorption by a strip of absorbing material,'' J. Acoust. Soc. Am. **11**, 396–400 (1940).
[7] A. Levitas and M. Lax, ''Scattering and absorption by an acoustic strip,'' J. Acoust. Soc. Am. **23**, 316–322 (1951).
[8] R. K. Cook, ''Absorption of sound by patches of absorbent materials,'' J. Acoust. Soc. Am. **29**, 324–329 (1957).
[9] T. D. Northwood, M. T. Geisaru, and M. A. Medcof, ''Absorption of sound by a strip of absorptive material in a diffuse sound field,'' J. Acoust. Soc. Am. **31**, 595–599 (1959).
[10] E. D. Daniel, ''On the dependence of absorption coefficients upon the area of the absorbent material,'' J. Acoust. Soc. Am. **35**, 571–573 (1963).
[11] F. P. Mechel, ''Iterative solutions for finite-size absorbers,'' J. Sound Vib. **134**, 489–506 (1989).
[12] F. P. Mechel, ''On sound absorption of finite-size absorbers in relation to their radiation impedance,'' J. Sound Vib. **135**, 225–262 (1989).
[13] P. M. Morse and K. U. Ingard, *Thoretical Acoustics* (McGraw-Hill, New York, 1968), pp. 454–463.
[14] S.-I. Thomasson, ''On the absorption coefficient,'' Acustica **44**, 266–273 (1980).
[15] A. de Bruijn, ''The sound absorption of an absorbing periodically uneven surfaces,'' Acustica **18**, 123–131 (1967).
[16] A. de Bruijn, ''Anomalous effects in the sound absorption of periodically uneven surfaces,'' Acustica **24**, 75–84 (1971).
[17] D. Takahashi, ''Excess sound absorption due to periodically arranged absorptive materials,'' J. Acoust. Soc. Am. **86**, 2215–2222 (1989).
[18] F. P. Mechel, ''Sound fields at periodic absorbers,'' J. Sound Vib. **136**, 379–412 (1990).
[19] D. Holmberg, P. Hammer, and E. Nilsson, ''Absorption and radiation impedance of finite absorbing patches,'' Acustica **89**, 406–415 (2003).
[20] I. N. Sneddon, *Mixed Boundary Value Problems in Potential Theory* (Wiley, New York, 1966), Chap. I, pp. 1–25.
[21] M. A. Celia and W. G. Gray, *Numerical Methods For Differential Equations* (Prentice–Hall, Englewood Cliffs, NJ, 1992), pp. 115–134.